

PAPER • OPEN ACCESS

Experimental investigation and numerical simulation of flow in the draft tube elbow of a Francis turbine over its entire operating range

To cite this article: M Sakamoto *et al* 2019 *IOP Conf. Ser.: Earth Environ. Sci.* **240** 072009

View the [article online](#) for updates and enhancements.

Experimental investigation and numerical simulation of flow in the draft tube elbow of a Francis turbine over its entire operating range

M Sakamoto¹, A Müller¹, L Andolfatto², T Hashii¹, K Yamaishi¹ and F Avellan²

¹ Nippon Koei Co., Ltd., Fukushima Works, 1-22 Doukyu, Aza, Morijyuku, Sukagawa, Fukushima Pref. 962-8508, Japan

² EPFL Laboratory for Hydraulic Machines, Avenue de Cour 33bis, 1007 Lausanne, Switzerland

E-mail: sakamoto-mh@n-koei.jp

Abstract. Hydraulic power plants are increasingly required to extend their operating range, enabling the seamless large scale integration of renewable energy sources into the electrical grid. In Francis turbines, the complex cavitation patterns appearing in the draft tube cone at off-design operation cause a decline in turbine performance and cyclic pressure pulsations that may lead to dangerous hydro-acoustic instabilities. The accurate prediction of the velocity distribution and the pressure pulsations by numerical simulation in the design phase is important for manufacturing stable and more efficient hydraulic machines over a wide operating range. This work seeks to improve the accuracy of numerical flow models for predicting the dynamic turbine characteristics through a systematic comparison of the velocity fields simulated with CFD and measured with Laser Doppler Velocimetry (LDV) in the draft tube cone. The numerical simulation and experimental measurements are performed in flow conditions for six values of discharge factor, four part load comprised 40%, 60%, 80%, 90% of the discharge value at the Best Efficiency Point (BEP), at the BEP, and one full load of 110%. The steady Reynolds-Averaged Navier-Stokes (RANS) simulation are performed for numerical analysis by the commercial flow solver ANSYS CFX. The LDV measurements are performed on a reduced scale model with a specific speed of $n_{QE}=0.20$, installed the test rig of EPFL Laboratory for Hydraulic Machines.

1. Introduction

Various types of cavitation patterns appear in the draft tube cone of Francis turbines at off-design operating conditions [1]. The consequences reach from a decline in turbine performance to critical instabilities. The accurate prediction of the cavitation characteristics, the velocity distribution and the pressure pulsations in the design phase is thus important for developing stable and more efficient hydraulic machines over a wide operating range. Commercial CFD tools provide a straight and increasingly used-friendly access to such analysis and are widely used in an industrial context, for instance for the refurbishment of existing small hydro power plants, where the performance of model tests is not always economical. Given the complexity of the flow, a validation of the numerical methodology with experiments is however important. The flow in the turbine at off-design operating points was investigated extensively in the recent past by measuring the velocity field with Laser



Doppler Velocimetry (LDV) and Particle Image Velocimetry (PIV) at deep part load, part load and full load in the frame of the HYPERBOLE research project [2, 3, 4, 5]. In a similar test case, the velocity field in the draft tube cone of a reduced scale Francis turbine model is investigated by LDV at six different operating points ($0.4, 0.6, 0.8, 0.9, 1.0$ and $1.1 \times Q_{\text{BEP}}$) and compared to the results from numerical simulations. More precisely, the axial (meridional) and tangential velocity profiles are established by performing LDV measurements at several radial positions between the cone wall and the cone centerline in a horizontal plane. They are then compared to the results of the steady state RANS simulations. The experimental and numerical setups are described in detail in Sections 2 and 3, while Section 4 includes the individual LDV and CFD results as well as a comparison between them. The outcome and the future work required to refine the numerical models is finally discussed in Sections 5 and 6.

2. Reduced scale model test

The reduced scale model tests were carried out on a Francis turbine with a specific speed of $n_{\text{QE}}=0.20$ (according to IEC standards [6]). The experimental setup on the test rigs of EPFL Laboratory for Hydraulic Machines is shown in Figure 1.

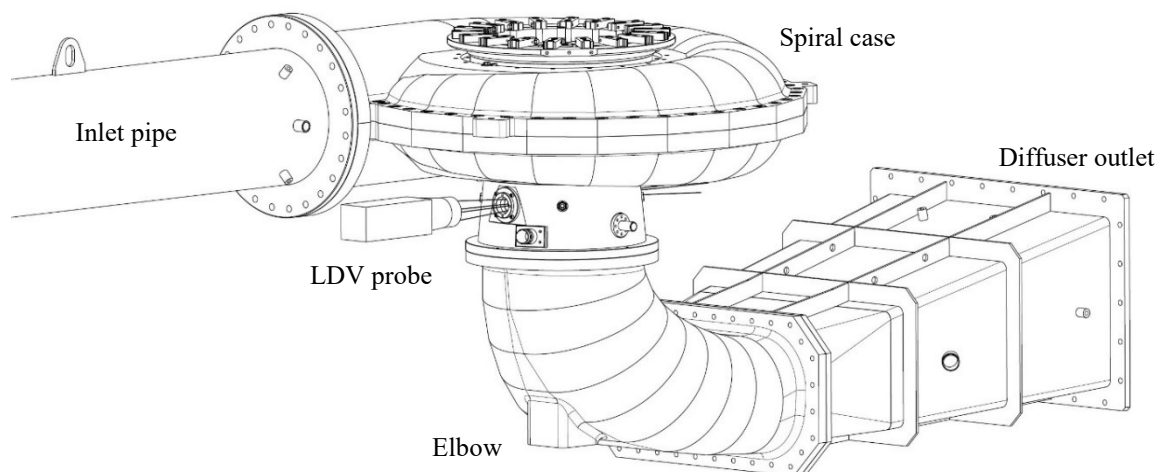


Figure 1. Reduced scale model of a Francis turbine with flow survey instrumentation.

2.1. Investigated operating conditions

The investigated operating conditions are summarized in Table 1. The measurements are performed for six values of the unit discharge factor Q_{11} , whereas the value of the unit speed factor n_{11} is kept constant at the BEP value. n_{11} and Q_{11} are defined in equation (1).

$$n_{11} = \frac{nD}{\sqrt{H}}, Q_{11} = \frac{Q}{D^2 \sqrt{H}} \quad (1)$$

Table 1. Investigated operating conditions.

	OP1 (Deep part load)	OP2 (Part load)	OP3 (Part load)	OP4 (Part load)	OP5 (BEP)	OP6 (Full load)
n_{11}	72	72	72	72	72	72
Q_{11}	0.326	0.49	0.653	0.734	0.816	0.898
$Q_{11} / Q_{11,\text{BEP}}$	0.4	0.6	0.8	0.9	1	1.1

2.2. Experimental setup

The flow velocity components are measured with Laser Doppler Velocimetry (LDV) in a horizontal cross-section of the draft tube cone, located at a distance of 245 (mm) from the reference level of the model turbine. The setup is shown in Figure 1 and 2. The LDV probe is mounted on a 2-D traversing system for displacements along the x and y axes. The draft tube cone radius of the measuring section is $R_{\max}=1.06 \times R_{\text{ref}}$. The axial and tangential velocity components are measured on 31 radial positions between the cone centerline and the cone wall along the x axis in 6 (mm) steps. A flat optical window is installed on the cone wall to avoid distortion errors caused by circularly shaped interfaces. Pressure fluctuations are measured simultaneously on the same measuring section of the draft tube cone at 90° intervals by dynamic pressure transducers. The pressure data is recorded with a PXI modular electronic instrumentation platform and the BSA (burst spectrum analyzer) determines the velocity components from the LDV probe in non-coincidence mode. The measurement requires a sufficient acquisition time to provide a stable average of the flow velocity. Observing the data during a continuous test run over 300 (s), this was achieved, without further prove, after 60 (s).

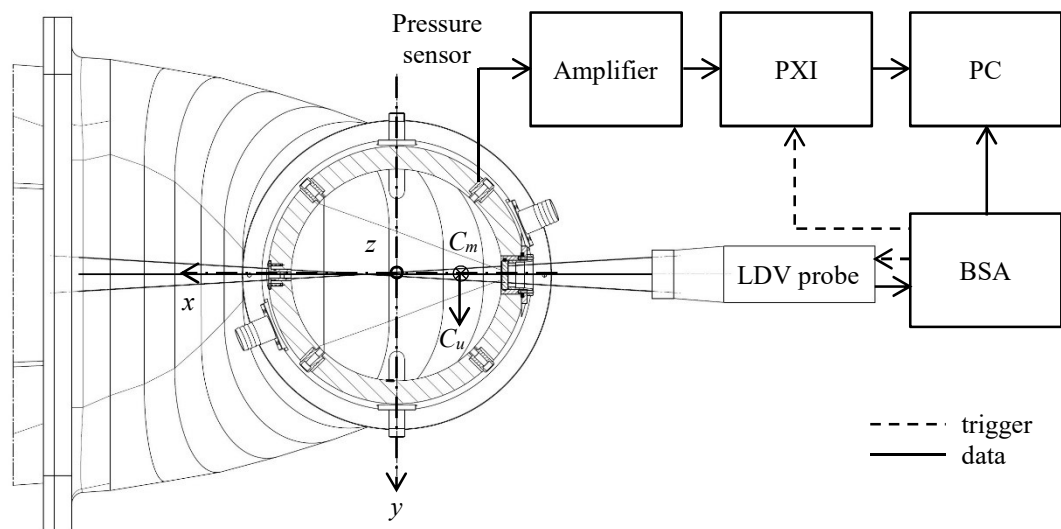


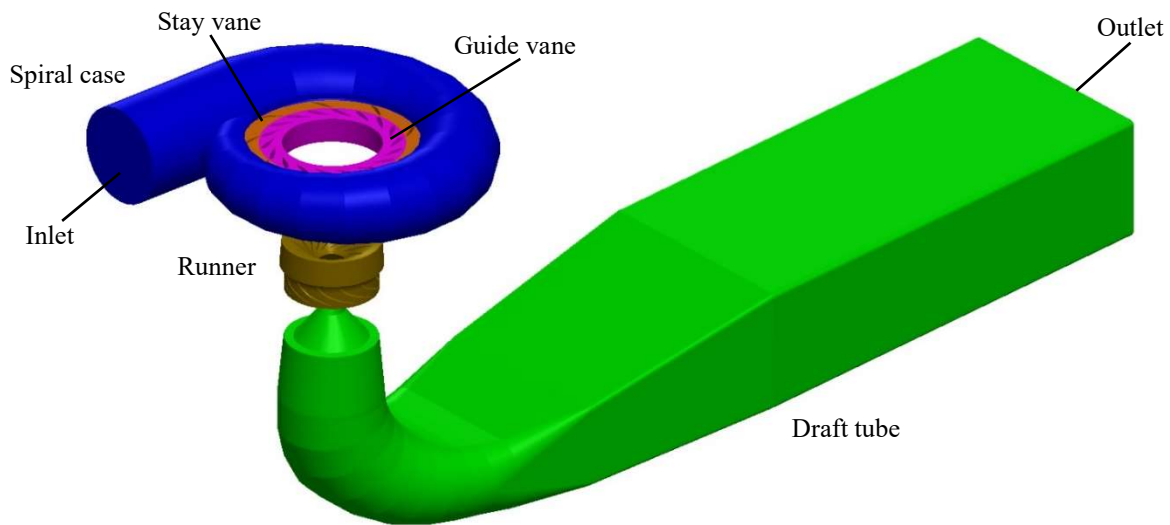
Figure 2. Setup for LDV measurement.

3. Numerical simulation setup

The mean velocity fields over the entire operating range were first calculated with the steady state RANS simulations and a structured hexahedral mesh using the commercial CFD code ANSYS CFX v18.2. Even though the efficiency was accurately predicted, the comparison of the velocity profiles with the LDV results was somewhat unsatisfactory and therefore it was decided to perform the transient simulation. Furthermore, changes were made to the mesh (from unstructured tetrahedral to structured hexahedral) and different boundary conditions were also tested.

3.1. Computing domain

The volume and surfaces of the spiral casing, the stay vane, the guide vane, the runner and the draft tube of the reduced scale model water passage are defined as the computing domain represented in Figure 3. All the components were meshed with a structured hexahedral topology using the commercial tool ANSYS ICEM CFD v18.2. The properties of this topology are defined in Table 2. This also includes an extension of the draft tube for flow stabilization.

**Figure 3.** Computing domain of NK F62 Francis turbine.**Table 2.** Properties of topology.

	Spiral casing	Stay vane	Guide vane OP5 (BEP)	Runner	Draft tube
Elements (structured hexahedral)	1,098,995	846,171	2,762,856	5,860,270	2,204,893

3.2. Simulation conditions

The parameters of the numerical simulations are summarized in Table 3. For the initial steady state simulations (#1-6), the stable pressure P_{in} based on the head was imposed at the spiral case inlet as a boundary condition. The outlet boundary condition at the draft tube exit was set as static pressure $P_{out} = 0$ (Pa) and an SST turbulence model was chosen for all simulations. The unit discharge factor Q_{11} was reproduced by setting the same guide vane opening angle as in the model test for each operating point. As previously mentioned, simulations #1-6 correspond to the operating conditions in Table 1, whereas simulations #7 and #8 were performed in order to assess the effect of the transient setups on the flow characteristics and convergent qualities. It was decided to run the transient simulations #7 and #8 based on the steady state simulation #5 at BEP, during 2 runner revolutions with a time step corresponding to roughly 10° iterations and roughly 1° iterations, respectively. RMS residual represents the highest RMS residual value of the velocity residuals at the last iteration.

Table 3. Parameters for the numerical simulations.

#	Type	P_{in} (Pa)	P_{out} (Pa)	Iterations	Steps	RMS residual
1-6	Steady State	$\rho g H$	0	10^4	-	$1e-5$
7	Transient (10°)	$\rho g H$	0	-	72	$1e-7$
8	Transient (1°)	$\rho g H$	0	-	720	$1e-8$

4. Results

4.1. Velocity profiles from LDV

The mean velocity profiles are shown in Figure 4. C_m and C_u represent the axial velocity component and the tangential velocity component, respectively. The measured C_m and C_u are made non-dimensional with the mean discharge speed C_Q and the circumferential runner velocity U defined as equation (2). $R/R_{\max}=0$ is the cone centerline and $R/R_{\max}=1$ is the cone wall. In the region close to the cone wall, the results for C_u sometimes do not contain enough data points for the statistical analysis. For OP5 (BEP) in Figure 4, C_m is approximately equal to the reference C_Q . For the off-design operating points, C_m declines towards the center of the cone due to the presence of a dead- or recirculation zone with a vortex rope. C_u also decreases towards the cone center and changes rotating direction to the opposite direction of the runner at OP5 (BEP) and OP6.

$$U = \frac{\pi DN}{60} \quad (2)$$

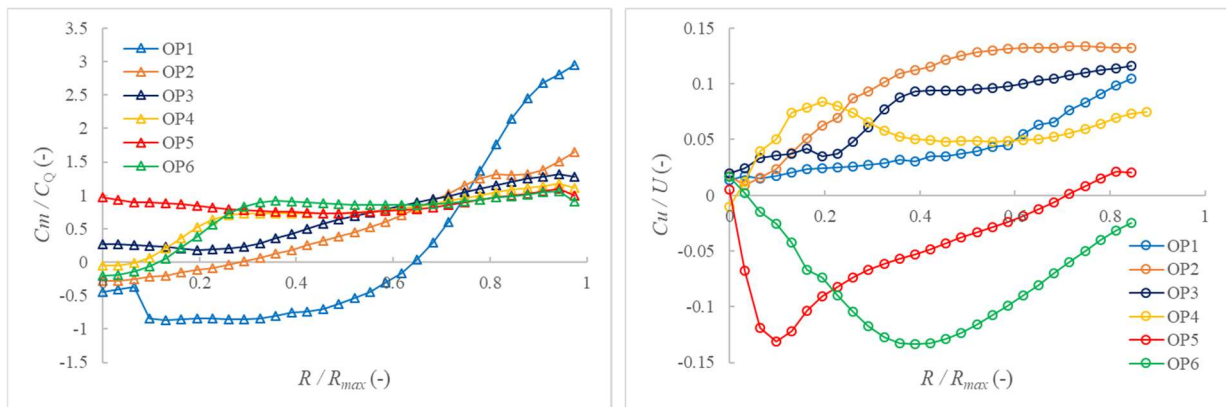


Figure 4. Experimental results of Axial velocity component C_m (left) and Tangential velocity component C_u (right) for 6 operating conditions.

4.2. Draft tube flow field from CFD

The velocity and pressure distributions in the draft tube obtained by the steady state simulations #1-6 are presented in Figure 5 and Figure 6, where the color bars in Figure 5 also apply to the graphs in Figure 6. These distributions are picked up from the same stream-wise measuring section of the draft tube cone as the LDV measurements.

5. Comparison of numerical simulation results with experimental data

5.1. Velocity profiles

Figure 7 shows the comparison of the C_m and C_u profiles for all operating points. For lower part load conditions, there is a good agreement between the experimental and the numerical data at OP1 (40%). At OP2 (60%), the axial velocity component C_m is significantly underestimated by the CFD in the central region of the cone and overestimated towards its wall. The same is true for the tangential velocity component C_u , where the differences are even more pronounced. For a higher part load regime at OP3 (80%), C_m and C_u are underestimated by the CFD in the central region of the cone. Close to the BEP at OP4 (90%), the numerically calculated C_u predicts the LDV profile rather poorly.

C_m is well reproduced beyond 30% of the cone radius toward the wall and significantly overestimated by the CFD results in the cone center. For the BEP at OP5, the qualitative behavior of the C_u curve is well reproduced by the CFD, the latter being however shifted by roughly 10% towards the cone wall. The CFD significantly underestimates C_m at the cone center and even displays a recirculation zone. For full load operation at OP6 (110%), the velocity curve shapes are well matched for both velocity components, with a negative offset for C_u (underestimation) and an underestimation of C_m in the cone center region by the CFD. Finally, Figure 8 contains the comparison of the C_m and C_u obtained by the steady state simulation and the transient simulation at OP5 (BEP). The results by the transient simulations still have the same characteristics as the steady state results, even though convergence was significantly improved between the two.

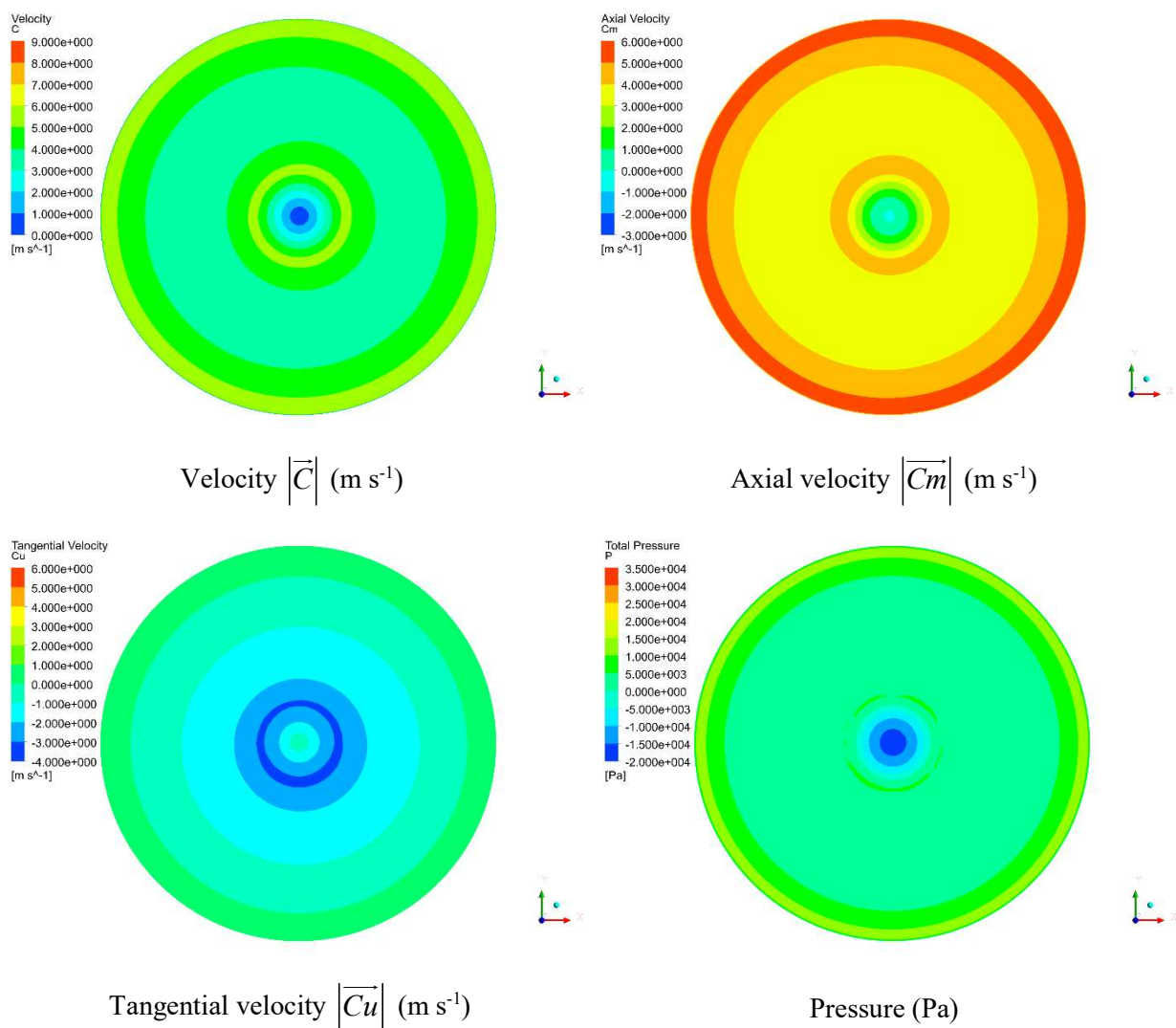


Figure 5. Velocity and pressure distributions in the measurement section at OP5 (BEP).

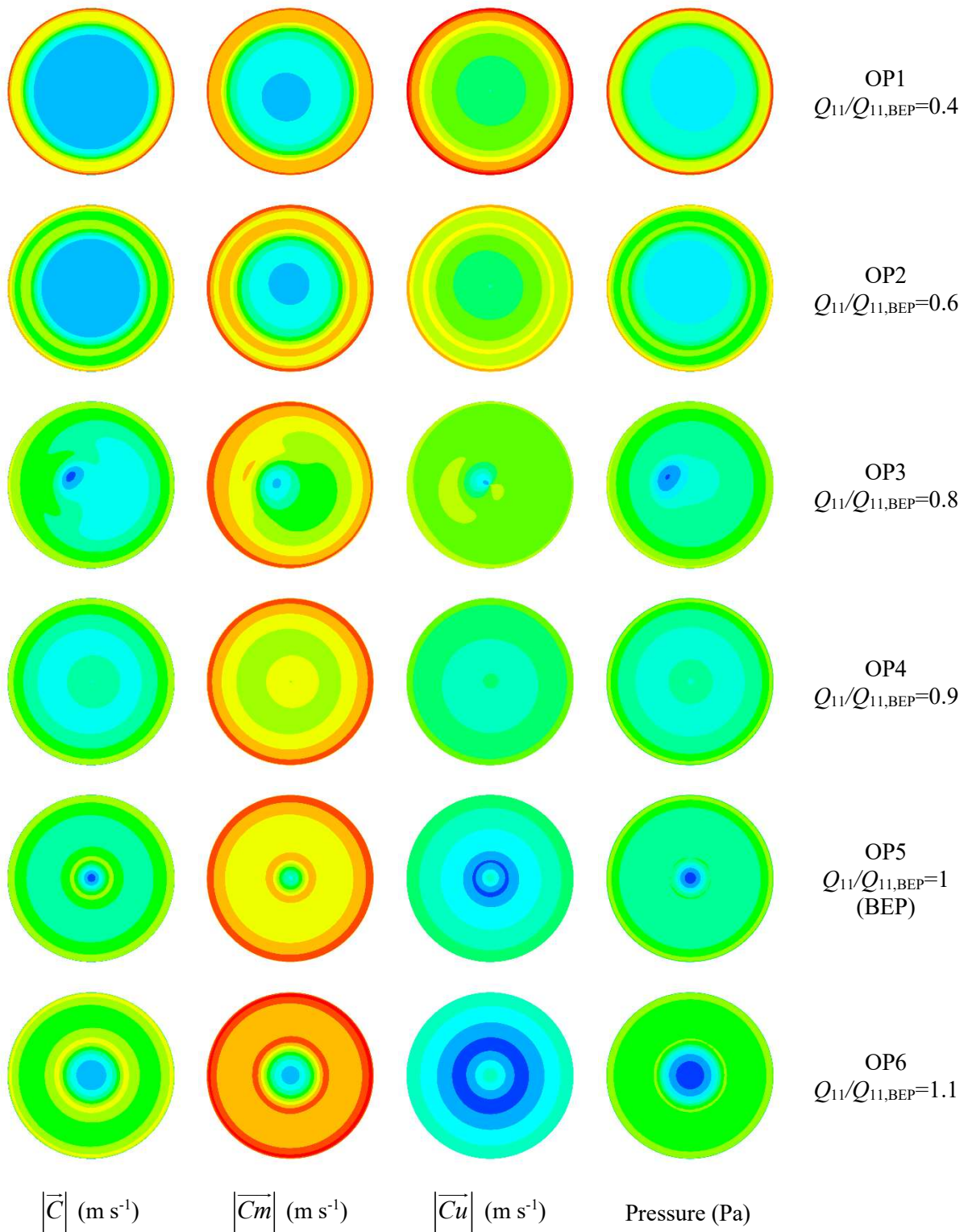


Figure 6. Velocity amplitude $|\vec{C}|$, Axial velocity component $|\vec{C}_m|$,

Tangential velocity component $|\vec{C}_u|$ and pressure distribution by numerical simulation.

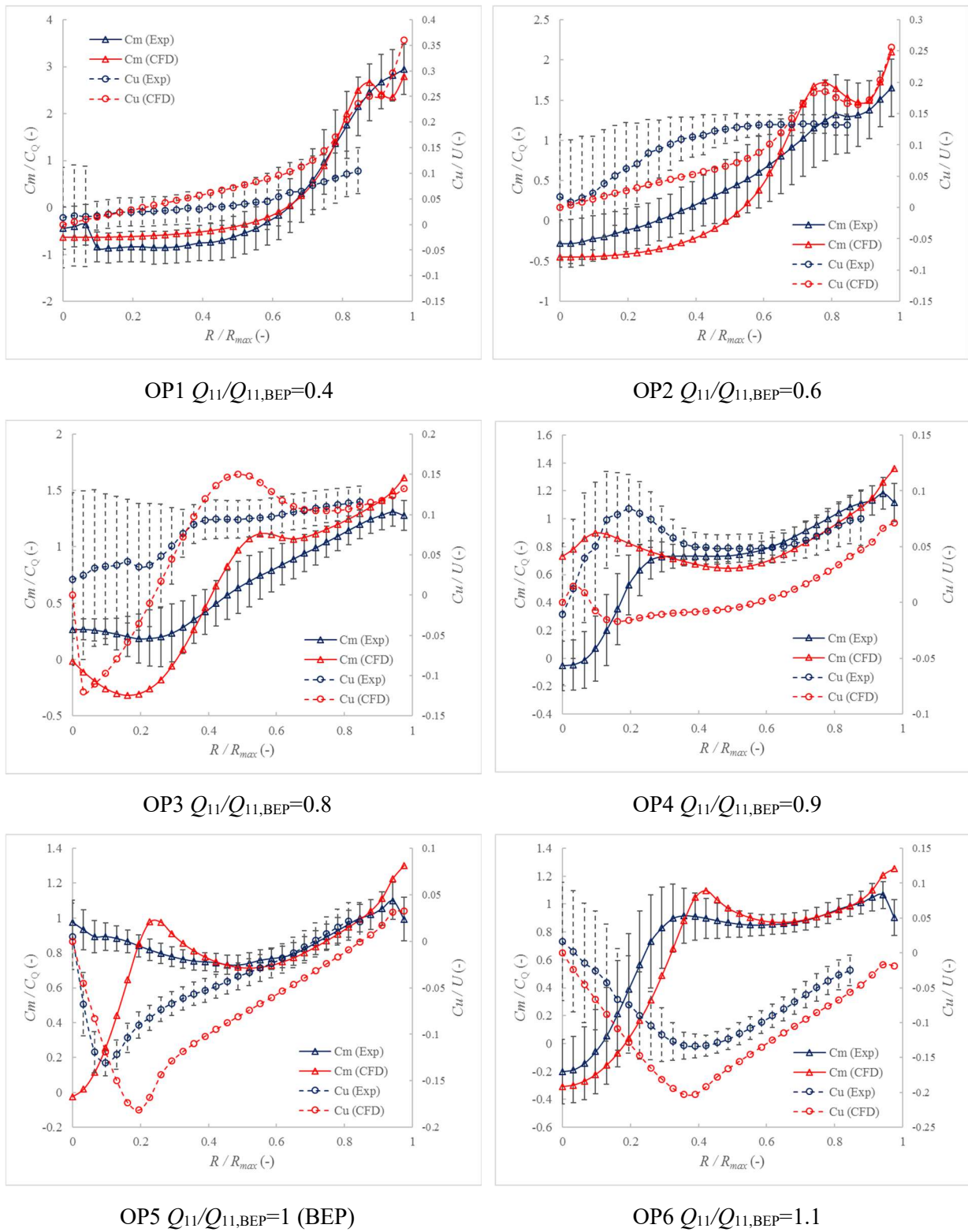


Figure 7. Velocity profiles by experiments and numerical simulations for 6 operating conditions.

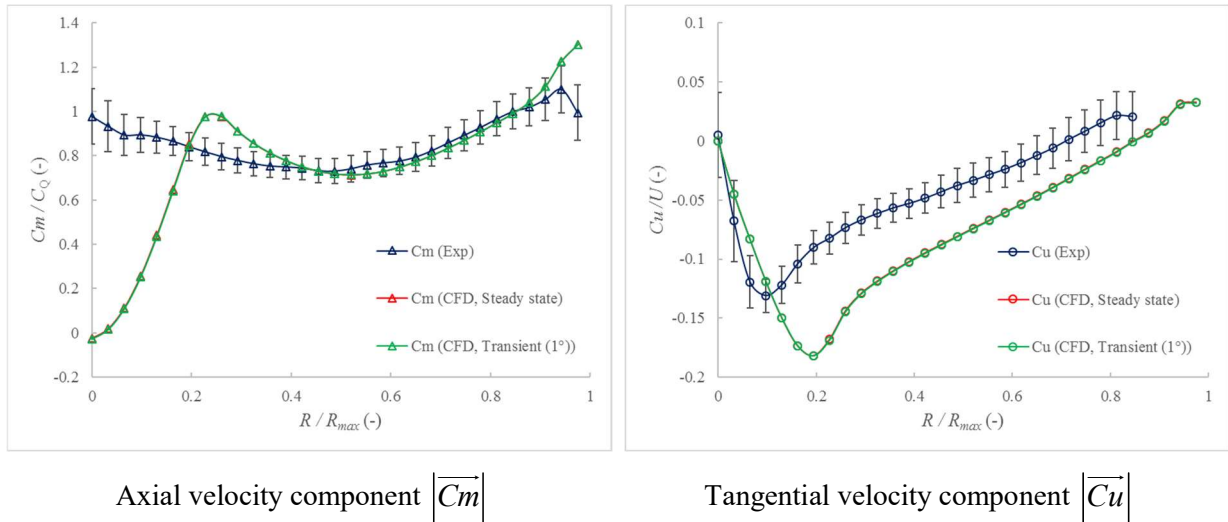


Figure 8. Velocity profiles by experiments, steady state numerical simulations and transient numerical simulations for BEP.

5.2. Turbine efficiency

The comparison of the turbine efficiency is shown in Figure 9 and 11. The measured efficiency values are slightly lower than the simulation results for part load conditions. The reason for this is that the leakage flow outside of the runner is not taken into account in the simulation, which is illustrated by the simulated discharge Q in Figure 11 in the lower range.

5.3. Mechanical torque

The comparison of the mechanical torque is shown in Figure 10 and 11. As in case of the efficiency, the measured values are slightly lower than the CFD result. One of the explanations is the influence of disk friction in the experimental measurement, where there are significant differences for part load conditions.

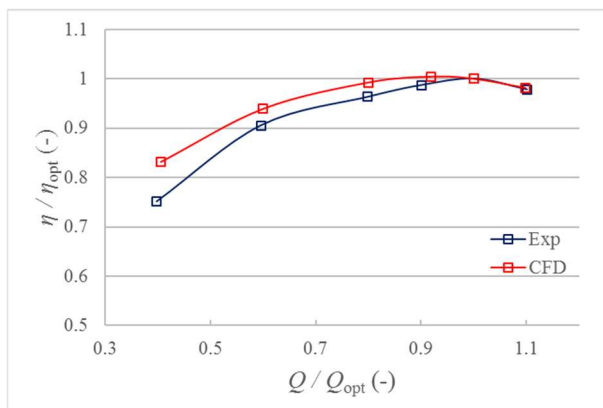


Figure 9. Turbine efficiency by experiments and numerical simulations.

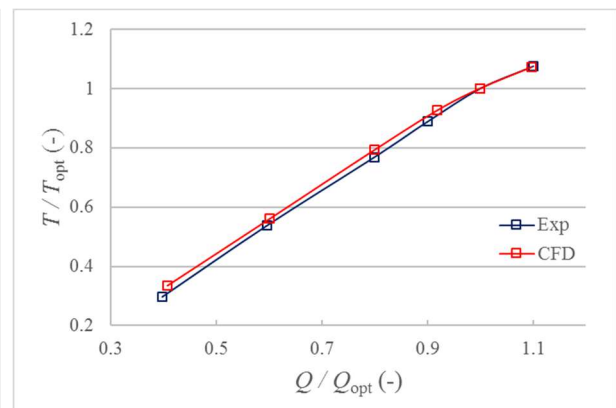


Figure 10. Mechanical torque by experiments and numerical simulations.

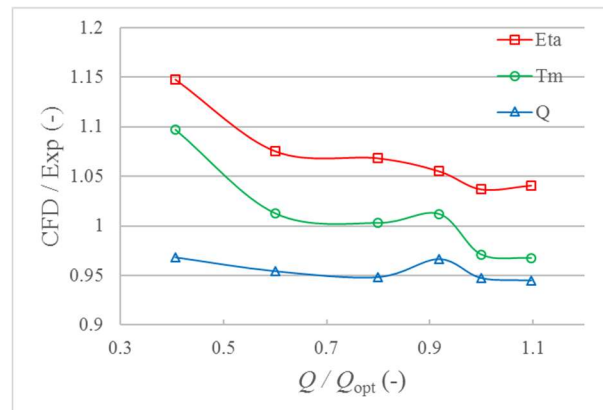


Figure 11. Comparison of values by experiments and numerical simulations.

6. Summary and discussions

The overall performance in terms of efficiency seems well reproduced by the CFD calculation across the entire operating range of the turbine and the differences at part load are possibly explained by not considering the leakage flow in the simulations. However, there are some significant differences in the draft tube flow velocity distributions between the CFD results and the experimental data obtained by LDV. The deviations are generally larger in the cone centre. Furthermore, the comparison between OP4 and OP5 suggests that the BEP does not occur at the same discharge judged by the residual swirl (tangential velocity component C_u) in the flow, which would explain some of the qualitative differences around this point. The role played by the numerical setup is currently being investigated.

7. Conclusion and perspectives

The performance of the reduced scale model of a Francis turbine over an extended operating range (40% - 110%) was simulated by CFD and compared to the data from model testing. In an objective of validating the numerical approach, axial and tangential velocity profiles were measured in the draft tube by LDV and systematically compared to the CFD output. While the overall efficiency was generally well predicted, quantitative and qualitative differences are revealed in the velocity distributions between the LDV and CFD results. The underlying reasons are currently being investigated by adjusting the numerical setup for the simulations. As the constitution of the draft tube flow is an important indication for the hydraulic performance and the potential risk of hydro-acoustic instabilities, its accurate prediction by CFD models is important. The results presented in this paper show that the current approach has to be refined to reflect this. Furthermore, the transient simulations will be performed and the analysis will be extended to include the cavitation characteristics in order to further improve the turbine design approach based on CFD.

Acknowledgements

The authors would like to acknowledge the commitment of the Laboratory for Hydraulic Machines' technical staff, especially Alain Renaud, Vincent Berruex, Benjamin Neuhaus, Monica Suarez and Georges Crittin.

Nomenclature

C_m	Axial velocity component (m s^{-1})	Q	Discharge ($\text{m}^3 \text{s}^{-1}$)
C_u	Tangential velocity component (m s^{-1})	Q_{11}	Specific discharge factor (-)
D	Runner outlet diameter (m)	R_{ref}	Runner reference radius (m)
E	Specific energy; $E=gH$ (J kg^{-1})	S	Swirl number (-)
g	Gravitational acceleration (m s^{-2})	T	Mechanical torque (Nm)
H	Head (m)	η	Turbine efficiency (-)
N	Rotational speed (min^{-1})	v	Specific speed (-)
n_{11}	Specific rotational speed factor (-)	ρ	Density (kg m^{-3})
P	Power (W)	σ	Thoma cavitation number (-)
p	Pressure (Pa)	ω	Angular velocity (s^{-1})

References

- [1] Avellan F. (2004), Introduction to Cavitation in Hydraulic Machinery, *The 6th International Conference on Hydraulic Machinery and Hydrodynamics*, Timisoara, Romania.
- [2] Müller A., Favrel A., Landry C., Avellan F. (2017), Fluid-structure interaction mechanisms leading to dangerous power swings in Francis turbines at full load, *Journal of Fluids and Structures* **69**, pp. 56-71.
- [3] Favrel A., Gomes J., Landry C., Müller A., Nicolet C., Avellan F. (2017), New insight in Francis turbine cavitation vortex rope: role of the runner outlet flow swirl number, *Journal of Hydraulic Research* (2017).
- [4] Favrel A., Müller A., Landry C., Yamamoto K., Avellan F. (2015), Study of the vortex-induced pressure excitation source in a Francis turbine draft tube by particle image velocimetry, *Experiments in Fluids* **56**(12).
- [5] Yamamoto K., Müller A., Favrel A., Avellan F. (2017), Experimental evidence of inter-blade cavitation vortex development in Francis turbines at deep part load conditions, *Experiments in Fluids* **58**(10).
- [6] IEC standards 60193 (1999), Hydraulic Turbines, Storage Pumps and Pump-Turbines - Model Acceptance Tests, 2nd edition. International Electrotechnic Commission, Geneva, Switzerland.
- [7] Maruzewski, P. (2010), Turbulence modeling for Francis Turbine water passages simulation, *The 25th IAHR Symposium on Hydraulic Machinery and Systems*, Timisoara, Romania.
- [8] EPFL Laboratory for Hydraulic Machines (2017), NK-F62 2nd Development Project Model Test Report, Lausanne, Switzerland (internal document).